Journal of Applied Mechanics and Technical Physics, Vol 38, No. 3, 1997

INSTABILITY OF A THREE-DIMENSIONAL BOUNDARY LAYER ON A SWEPT WING

V. Ya. Levchenko and V. A. Scherbakov

UDC 532.526

Evolution of steady vortices in a three-dimensional boundary layer was first noted by Gray in experiments [1]. In [2], having developed a linear stability theory for a three-dimensional boundary layer, Stuart substantiated this phenomenon theoretically. A canonical three-dimensional boundary layer is formed, in particular, in flow about the so-called swept wing of infinite span.

The flow pattern about an airfoil at incidence is presented in Fig. 1, where 1 is the potential-flow streamline. The streamline is curved in the regions of favorable streamwise pressure gradients (flow acceleration) in the front part of the airfoil and in the regions of adverse pressure gradients in approaching the trailing edge, the centrifugal forces being balanced by the corresponding pressure gradients in the direction of streamline concavity. These gradients remain in the boundary layer, while the centrifugal forces decrease on approaching the wall owing to viscous friction. As a consequence, secondary flows which are perpendicular to the potential streamline toward its concavity (direction 2 in Fig. 1) arise in the boundary layer. With zero values at the wall and outside the boundary layer, the velocity profile in this direction has an inflection point and is very unstable, according to the linear theory. The calculations carried out by Gregory et al. [2] and also in other studies have shown that the most unstable disturbances are the waves of zero frequency, i.e., steady vortices whose axes are directed approximately along the potential streamline for the case of swept wings. In the last decade, many theoretical and experimental investigations have been aimed at studying the development and properties of steady vortices caused by the instability of secondary flows [3–6].

Considerably less attention has been paid to travelling waves which are also developed owing to the instability of secondary flows. Until recently, the experimental material was presented only by DLR researchers (Germany) [7–10]. The experiments were carried out under the so-called "natural" conditions, i.e., under conditions of operation of a wind tunnel without artificial (controlled) wave excitation. Some qualitative features of transition to turbulence, in particular, the relative role of steady vortices and travelling waves, depending on the degree of turbulence of the incoming flow, the periodic variation in the spanwise amplitude of travelling waves, etc. were revealed. However, nonlinear effects manifested themselves in these experiments as early as the instability waves were registered, and the rates of growth of both types of instability waves differed substantially from those predicted by the linear theory.

The recent experiments in [11–14] have been carried out under "natural" conditions as well, except for [15], with the use of various measurement techniques. That is why the experimental results agree in some aspects but contradict one another. One should note the existence of another type of travelling waves. These waves are caused by the secondary instability of steady vortices whose frequencies are an order of magnitude higher than the frequencies of travelling instability waves of the secondary flow [12–14]. Their development begins near the boundary-layer edge, while the primary instability waves are generated near the surface.

At present, experimental data are being accumulated the deficiency of which does not allow one to use confidently one or another technique for calculating the point of transition to turbulence in three-dimensional boundary layers [16].

Institute of Theoretical and Applied Mechanics, Siberian Division, Russian Academy of Sciences, Novosibirsk 630090. Translated from Prikladnaya Mekhanika i Tekhnicheskaya Fizika, Vol. 38, No. 3, pp. 32–38, May–June, 1997. Original article submitted February 26, 1996.

0021-8944/97/3803-0357 $18.00

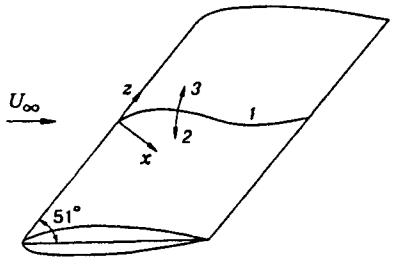

Fig. 1

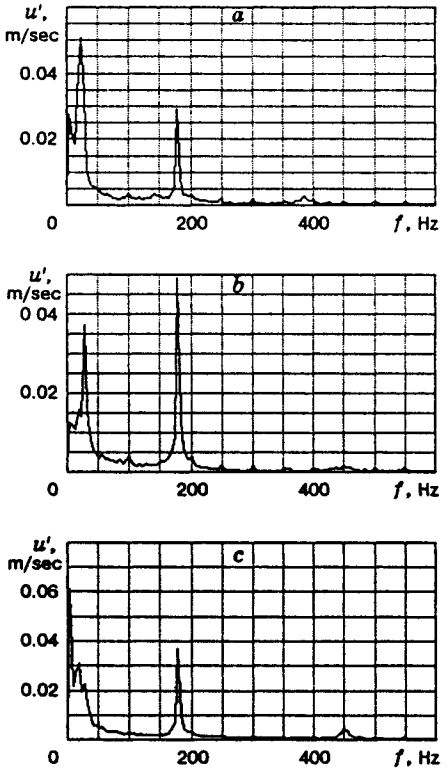

Fig. 2

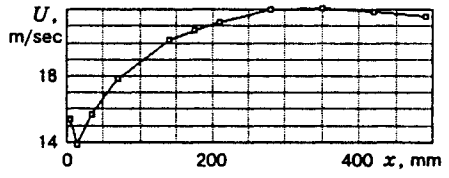

Fig. 3

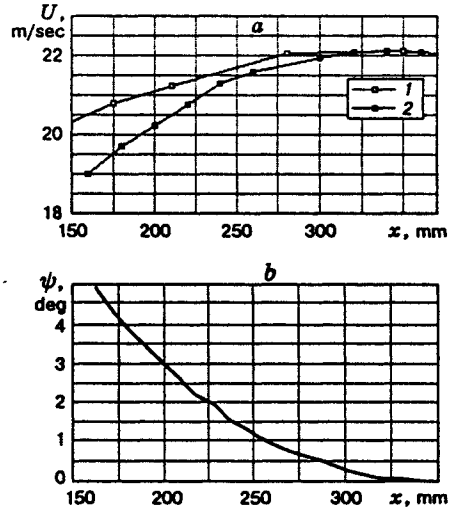

Fig. 4

The present paper is devoted to obtaining additional experimental information. It differs from the previous studies by artificial excitation of travelling waves of a given frequency which is, contrary to [15], not localized.

Experiments were carried out in a T-324 low-turbulent wind tunnel at the Institute of Theoretical and Applied Mechanics, Siberian Division, Russian Academy of Sciences. The swept-wing model had a chord with a length of 700 mm (in the x direction in Fig. 1), a 1120-mm span in the z direction, a maximum wing thickness of 15%, and a leading-edge sweep angle of 39°. The model was mounted vertically in the test section. We performed measurements using a hot-wire anemometer DISA 55M01. The hot-wire probe was aligned parallel to the leading edge. The hot-wire signals were entered into a Macintosh Classic II personal computer for subsequent processing. All data were obtained in the course of the experiment on the basis of ten realizations. The measurements were done through a 400-mm-diameter window located in the side wall of the test section. The basic measurements were performed within the range of $160 \leqslant x \leqslant 360$ mm.

The pressure distribution along the chord was measured in a standard manner through orifices located at a distance of 10 mm from the section of basic measurements along the x axis. The spanwise measurements (along the z axis) were carried out in the cross section $x = 275$ mm. Travelling waves of a fixed frequency were excited in the boundary layer using a loudspeaker placed downstream of the model.

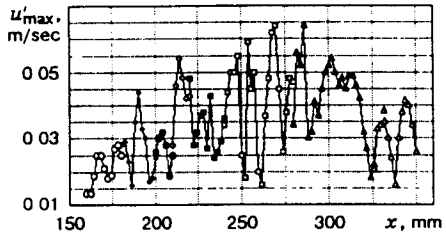

Fig. 5

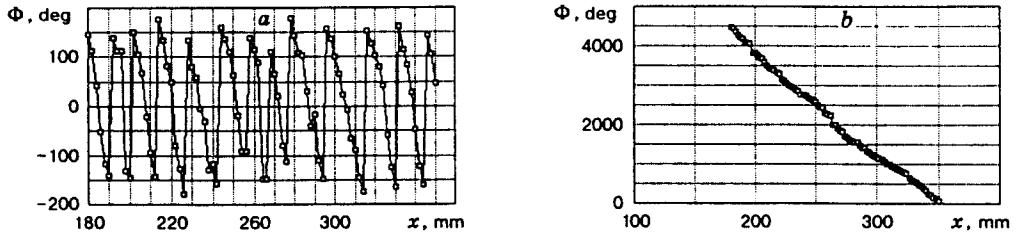

Fig. 6

The experimental regime that we chose for measurements was such that the development of both naturally and artificially excited travelling waves occurred in the linear region. Figure 2 shows the spectra measured at the characteristic points inside the boundary layer at the beginning (a), in the middle (b), and at the end (c) of the measurement region. The disturbance frequencies f are plotted as the abscissas, and their root-mean-square values u' are plotted as the ordinates. The values of u' were measured with filtration of signals in a 4-Hz band. The free-stream velocity was 20.2 m/sec, and the angle of attack of the model was $\approx -10°$. As is seen from Fig. 2, the natural wave packet had a central frequency of $\approx$30 Hz under these conditions. The excited wave frequency which lies below the frequency range of secondary instability waves was equal to 178 Hz, which was far enough from the frequency range of the natural wave packet to avoid an increase in its amplitude up to the nonlinear level. It is seen from Fig. 2 that both the natural wave packet and the excited wave had fairly low amplitudes excluding their combinative interaction. The amplitude of the excited wave increases slightly in the middle of the measurement region and decays at the end of it, which is typical of passage of the curve of neutral stability of the linear theory. The twofold change of the sound amplitude caused the twofold change of the wave amplitude, which is also indicative of the linearity of the process. In the remaining figures, the data on disturbance characteristics are presented for a frequency of 178 Hz. The mean and fluctuating velocities were measured with a step of 2 mm in the streamwise direction x and with a step of 1 mm in the spanwise direction z.

Figure 3 shows the distribution of the potential flow velocity along the wing chord calculated using the measured pressure distribution. The region of basic measurements was affected by favorable pressure gradients, except for the last 50–60 mm.

Figure 4a shows velocity distributions outside the boundary layer in the measurement region obtained with the use of the pressure distribution (points 1) and hot-wire measurements (points 2). Points 1 are the values of the velocities directed along the potential-flow streamline, and points 2 are the velocity-vector components in the free-stream direction U_∞. The change of the angle of streamline inclination ψ to the direction of U_∞ in the measurement region is shown in Fig. 4b.

Figures 5 and 6 show the distributions of the disturbance amplitudes u'_{max} and phases Φ [u'_{max} are the maximum values of u' in the profiles $u'(y)$, where y is the distance from the model surface]. In Figs. 5 and 6a, one can see the periodicity of the disturbance field which is connected with the existence of steady vortices, because the measurements were performed with crossing of the system of these vortices.

Figure 7 shows schematically a pair of adjacent vortices induced by the instability of secondary flows. The arrows indicate the directions of vortex rotation and distributions of the vertical components of the mean velocities. In the regions where the high-speed fluid from the outer part of the boundary layer penetrates into the inner part, the flow is more stable than in the regions where, having been decelerated near the surface,

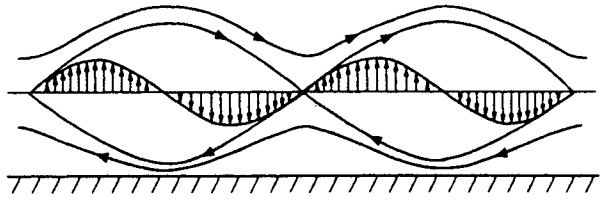

Fig. 7

the fluid is entrained into the external layers. This determines the presence of maxima and minima in the $u'(x)$ distribution in Fig. 5.

It should be noted that different points show the results obtained at different times and in different days and, hence, point to good reproducibility of the experimental results. The region of generation of both steady vortices and travelling waves is obviously in the vicinity of the region of the beginning of measurements. The quantities $u'_{\max}$ at the minimum points are practically equal to the level of external disturbances ($u' = 0.12$–0.14 m/sec and $u'/U_\infty \approx 0.06\%$), which are acoustic waves. Steady vortices generated under noncontrolled conditions on the natural surface roughness are known to be nonuniform in intensity at the beginning of their evolution, though the periodicity is quite noticeable. This is obviously the reason for a scatter of the points of maxima (and other similar points) in the vicinity of $x = 200$ mm in Fig. 5. As the vortices are developing, their intensities tend to become equal, and this manifests itself in an appropriate behavior of the amplitude of travelling waves in the region $x \approx 250$ mm. The general tendency of $u'_{\max}(x)$ behavior is typical of the development of waves in the region of instability and passage of the second branch of the neutral-stability curve of the linear theory. Estimation of the wavelength λ_x from 20 points of Fig. 5 and 23 points of Fig. 6a gave very close values (difference 0.5 mm) and its mean value was equal to 13.5 mm. Figure 6b shows the data from Fig. 6a with addition of 360° after each phase jump. The two figures show that the x component of the phase wave velocity c_x is directed toward the leading edge.

Figure 8 shows the mean-velocity distribution in the transversal direction z which was measured at a constant distance from the surface. Along the curve $y = \text{const}$, one can notice the flow periodicity, but there is a scatter in velocity-defect values, as was mentioned above. Figure 9 shows a spanwise z distribution of the maximum values of the disturbance amplitudes taken from the measured profiles $u'(y)$. Figures 10 and 11 show the curves of equal amplitudes and defects of the mean velocities, respectively, representing the general vortex structure of the boundary layer. The periodicity of both the mean flow and the field of disturbances is pronounced. The plus sign in Fig. 11 indicates the fluid motion toward the surface, and the minus sign indicates the reverse direction. The maximum values of the mean velocity defect in the region (+) correspond to the minimum values of the maximum amplitudes of disturbances in Fig. 9, and those in the region (−) correspond to the maximum values of $u'_{\max}$.

Figure 12 shows the variation in the disturbance phase in the spanwise direction. One can see that the corresponding phase-velocity component c_z is directed toward positive z. The wavelength λ_z estimated from Figs. 9 and 12 equals ≈ 9.1 mm. Since λ_x and λ_z are the components of the disturbance wavelength with a frequency of 178 Hz, the corresponding phase-velocity components c_x and c_z are equal to 2.4 and 1.65 m/sec. In [11], the direction of the wave vector k was determined as the direction perpendicular to a straight line connecting the ends of the vectors c_k which are the components of the vector c in different directions relative to the potential streamline. Two directions are obviously sufficient for this procedure. Following this procedure and using the data presented in Fig. 4, one can show that under these experimental conditions the wave propagates at an angle of 78° to the potential streamline in a direction opposite to the secondary flow (direction 3 in Fig. 1). In experiments carried out under natural conditions [11, 13], the most unstable disturbances, which were determined by different methods, propagated approximately at an angle of 90° to the potential streamline. In this case, the excited wave had a frequency different from the frequencies of the natural-wave train (see Fig. 2). It was found in [15] that the direction of wave propagation depends substantially on the frequency. The phase velocity c was 1.17 m/sec (or $c/U_\infty \approx 0.06$). This result can be compared with the results obtained by other authors: $c/U_\infty \approx 0.07$ in [14] and $c/U_\infty \approx 0.04$–0.07 in [11].

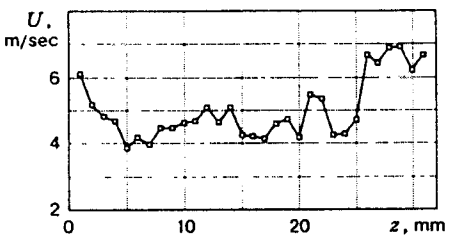

Fig. 8

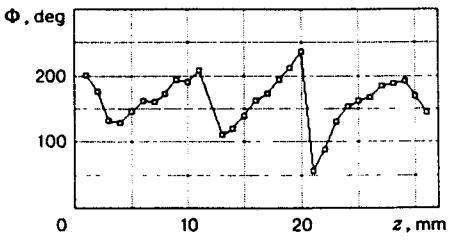

Fig. 12

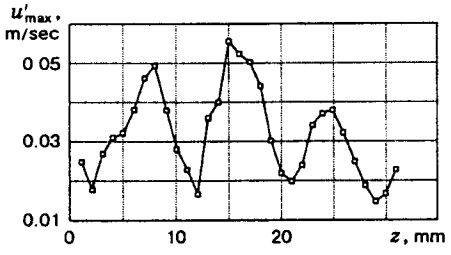

Fig. 9

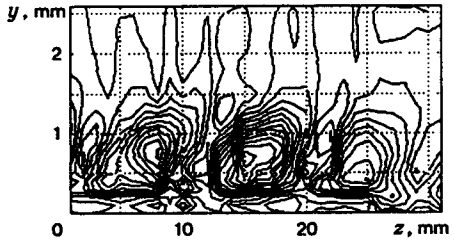

Fig. 10

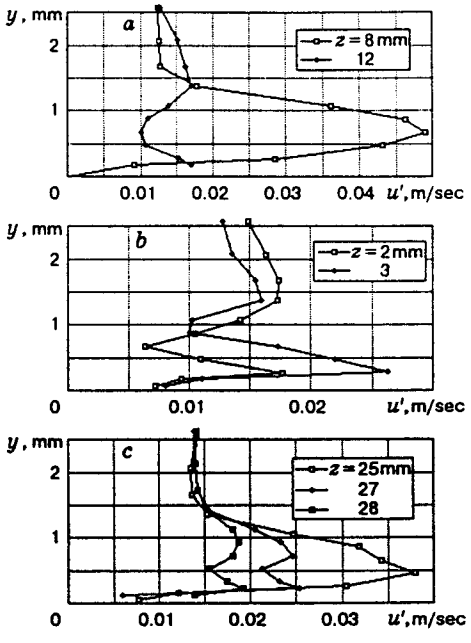

Fig. 13

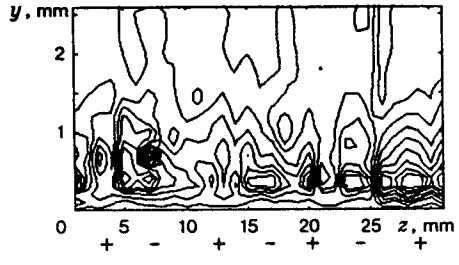

Fig. 11

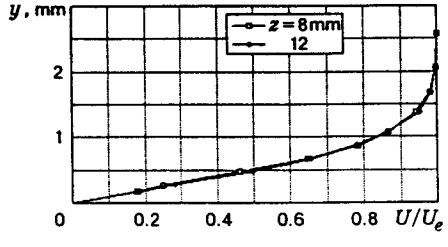

Fig. 14

The typical profiles of disturbance amplitudes are plotted in Fig. 13. Figure 13a shows the profiles $u'(y)$ in adjacent maximally unstable and stable cross sections (see Figs. 9 and 11). The profile $u'(y)$ for $z = 8$ mm has a shape typical of the disturbance profile of the travelling instability waves of the secondary flow [15, 16], and, for $z = 12$ mm, it has a specific shape with two maxima. The behavior of $u'(y)$ in the outer part of the boundary layer is typical of the amplification of an acoustic wave (Stokes' layer) with its subsequent viscous decay. However, generation of secondary-flow instability waves with maximum amplitudes near the wall begins in the inner region of the boundary layer.

The mean velocity profiles in Fig. 14 give an idea on the boundary-layer thickness and also the positions of $u'(y)$ maxima across the boundary layer. Figure 13b shows profiles in moving from the stable region (+) to the unstable one (−), and the reverse motion [from the unstable region (−) to the stable one (+)] is shown in Fig. 13c; the typical profile shape is the same. In moving from region (+) to region (−) (passing from the $z = 2$ mm section to the $z = 3$ mm section), the influence of the generated wave is extended from the distance $y \approx 0.65$ mm to $y \approx 1$ mm. In moving from the unstable region (−) to the stable one (+) (from $z = 25$ mm to $z = 28$ mm), the role of acoustic wave increases, with a shift of the first maximum with increasing distance from the surface.

Thus, we have obtained experimental data on the structure of a three-dimensional boundary layer on a swept-wing model under conditions of natural generation and development of steady vortices with artificial excitation and subsequent linear evolution of the travelling instability waves of secondary flow.

This work was supported by the Russian Foundation for Fundamental Research (Grant No. 96-01-01778).

REFERENCES

1. W. E. Gray, "The nature of the boundary-layer flow at the nose of a swept wing," in: RAE TM Aero255, Farnborough (1952).
2. N. Gregory, J. T. Stuart, and W. S. Walker, "On the stability of three-dimensional boundary layers with application to flow due to a rotating disk," *Philos. Trans. R. Soc. London*, **A248**, 155–199 (1955).
3. V. V. Kozlov (ed.), *Laminar–Turbulent Transition*, Springer-Verlag, Berlin (1985).
4. D. Arnal and R. Michel (eds.), *Laminar–Turbulent Transition*, Springer-Verlag, Berlin (1990).
5. R. Kobayashi (ed.), *Laminar–Turbulent Transition*, Springer-Verlag, Berlin (1995).
6. H. L. Reed and W. S. Saric, "Stability of three-dimensional boundary layers," *Annu. Rev. Fluid Mech.*, **21**, 235–284 (1989).
7. H. Bippes and P. Nitsche-Kowsky, "Experimental study of instability modes in a three-dimensional boundary layer," AIAA Paper No. 87-1335 (1987).
8. B. Müller and H. Bippes, "Experimental study of instability modes in a three-dimensional boundary layer," in: Proc. Symp. on Fluid Dynamics of Three-Dimensional Shear Flows and Transition, October 3–6, 1988, Chesme, Turkey.
9. B. Müller, "Experimental study of travelling waves in a three-dimensional boundary layer," in: D. Arnal and R. Michel (eds.), *Laminar–Turbulent Transition*, Springer-Verlag, Berlin (1990), pp. 489–498.
10. H. Bippes, "Experiments on transition in three-dimensional accelerated boundary layer flows. Invited paper," in: Int. Conf. on Boundary Layer Transition and Control, April 8–12, 1991, Cambridge, UK.
11. H. Deyhle, G. Hohler, and H. Bippes, "Experimental investigations of instability waves propagation in a three-dimensional boundary layer," *AIAA J.*, **31**, No. 4, 637 (1993).
12. Y. Kohama, W. S. Saric, and J. A. Hoos, A high frequency, secondary instability of crossflow vortices that leads to transition, in: *Boundary Layer Transition and Control*, Royal Aeronautical Society, Cambridge (1991), pp. 4.1–4.13.
13. Y. Kohama and D. Motegi, "Travelling disturbance appearing in boundary layer transition in a yawed cylinder," *Exp. Therapy. Fluid Sci.*, **8**, No. 4, 273–278 (1994).

14. Y. Kohama, Y. Kodashima, and H. Watanabe, "Randomization process in crossflow instability dominant three-dimensional boundary-layer transitions," in: R. Kobayashi (ed.), *Laminar-Turbulent Transition*, Springer-Verlag, Berlin (1995), pp. 455–462.
15. V. R. Gaponenko, A. V. Ivanov, and Y. S. Kachanov, "Experimental study of swept-wing boundary layer stability relative to unsteady disturbances," *Teplofiz. Aeromekh.*, **2**, No. 4, 333–359 (1995).
16. D. Arnal, G. Gasalis, and J. C. Juillen, "A survey of the transition prediction methods: from analytical criteria to PSE and DNS," in: R. Kobayashi (ed.), *Laminar-Turbulent Transition*, Springer-Verlag. Berlin (1995), pp. 3–14.
17. V. Ya. Levchenko and V. A. Scherbakov, "On 3-D boundary layer receptivity," *ibid.*, pp. 525–532.